

# RSC Advances



This is an *Accepted Manuscript*, which has been through the Royal Society of Chemistry peer review process and has been accepted for publication.

*Accepted Manuscripts* are published online shortly after acceptance, before technical editing, formatting and proof reading. Using this free service, authors can make their results available to the community, in citable form, before we publish the edited article. This *Accepted Manuscript* will be replaced by the edited, formatted and paginated article as soon as this is available.

You can find more information about *Accepted Manuscripts* in the [Information for Authors](#).

Please note that technical editing may introduce minor changes to the text and/or graphics, which may alter content. The journal's standard [Terms & Conditions](#) and the [Ethical guidelines](#) still apply. In no event shall the Royal Society of Chemistry be held responsible for any errors or omissions in this *Accepted Manuscript* or any consequences arising from the use of any information it contains.



## ARTICLE

## Surface functionalization of titanium with tetracycline loaded chitosan-gelatin nanosphere coatings *via* EPD: fabrication, characterization and mechanism

Received 00th January 20xx,  
Accepted 00th January 20xx

DOI: 10.1039/x0xx00000x

[www.rsc.org/](http://www.rsc.org/)

Xinjie Cai,<sup>†a</sup> Kena Ma,<sup>†ab</sup> Yi Zhou,<sup>ab</sup> Tao Jiang<sup>\*ab</sup> and Yining Wang<sup>\*ab</sup>

Biomedical metallic materials, such as titanium and stainless steel, have already been used in clinic and tissue engineering field for many years. However, the bio-inert surface limited and challenged their applications. The present study aimed to fabricate and characterize chitosan-gelatin (CSG) nanosphere based antibacterial coatings for surface functionalization of biomedical metallic materials. CSG nanosphere coating was fabricated on titanium substrate *via* electrophoretic deposition (EPD). Tetracycline (Tc), as a model functional agent, was loaded into the coating during fabrication. The mechanism of fabricating Tc loaded CSG nanosphere coatings *via* EPD was investigated for the first time. Characterization of the coatings showed nanosphere structure, and nanospheres can be released from the coatings. The entrapment of Tc was confirmed by fluorescent microscope, Fourier transform infrared spectroscopy and X-ray diffraction. It could also prove new hydrogen bonds formed between Tc and gelatin, as well as the increased crystallinity of the coating. Mechanical test demonstrated enhanced mechanical interlocking in the coating-titanium interface of high Tc concentration group. After coating preparation, the antibacterial effect of Tc was preserved both qualitatively and quantitatively. These results suggested that Tc loaded CSG nanosphere coating could be successfully fabricated *via* EPD, and used for the functionalization of titanium substrate. CSG nanosphere coating loaded with other functional agents would be a promising surface functionalization strategy for biomedical metallic materials.

### Introduction

Biomedical metallic materials, such as stainless steel, cobalt-based alloy, titanium (Ti) and its alloy, have the longest history among the various biomaterials.<sup>1, 2</sup> Owing to their excellent mechanical property and biocompatibility with human tissues, these metallic implants and scaffolds have been developed into key materials for biomedical applications in recent years,<sup>3, 4</sup> including the endosseous implants and bone fixation devices in dental and orthopaedic surgery; stent and heart valves in cardiovascular surgery; implanted electrodes in neurosurgery; and metallic scaffold in bone tissue engineering. However, due to the inertness of metallic surface, traditional metallic materials do not possess bio-function, and are associated with certain clinical challenges: bacterial infections, high failure rate in compromised condition, and extra systemic treatment.<sup>5, 6</sup> To overcome the drawbacks of inert metallic surface, a variety

of strategies have been developed. For example, plasma spraying has been used to fabricate alumina–nanosilver coating on titanium substrate.<sup>7</sup> Results showed favourable antibacterial property, but the high sintering temperature (800 °C) limited its application. Likewise, a molecular precursor method has been used to prepare hydroxyapatite coating on titanium mesh, which showed enhanced osteoblast activity and bone regeneration.<sup>8</sup> But the use of high temperature and organic solvent restricted its incorporation with other biological agents. Moreover, layer-by-layer technique has been employed to prepare hyaluronic acid and chitosan multilayers on titanium foil. After that, cell-adhesive arginine-glycine-aspartic acid (RGD) peptide was immobilized on the coating by protein immobilization.<sup>9</sup> This biopolymer coating could improve osteoblast proliferation and inhibit bacteria adhesion, but the preparation procedure was very complex. In summary, the physicochemical, morphological or biological properties of biomedical metallic materials could be upgraded to some extent after surface modification using suitable technology. Still, some weaknesses have limited their biomedical applications, such as severe preparation conditions (high temperature, organic solvent, radiation) that hinder the incorporation of biological agents, specific requirements for the substrate that restrict their applications on different shaped or three-dimensional (3D) complex structure, inadequate mechanical bonding in the substrate-coating interface, and poor stability of the loaded biological agents.<sup>10-</sup>

<sup>a</sup> The State Key Laboratory Breeding Base of Basic Science of Stomatology (Hubei-MOST) and Key Laboratory of Oral Biomedicine Ministry of Education, School and Hospital of Stomatology, Wuhan University, Wuhan 430079, China

<sup>b</sup> Department of Prosthodontics, Hospital of Stomatology, Wuhan University, Wuhan 430079, China

<sup>†</sup> Both authors contributed equally to this study.

\* Corresponding authors at: The State Key Laboratory Breeding Base of Basic Science of Stomatology (Hubei-MOST) and Key Laboratory of Oral Biomedicine Ministry of Education, School and Hospital of Stomatology, Wuhan University, 237 Luoyu Road, Wuhan 430079, China. Tel: +86 27 87686318; Fax: +86 27 87873260. Email addresses: jiangtao2006@whu.edu.cn and wang.yn@whu.edu.cn

<sup>12</sup> Therefore, further investigation for the advanced surface functionalization strategy is required.

According to literature, electrophoretic deposition (EPD) has been gaining increasing interest as an economical and versatile processing technique for the preparation of novel bioactive coatings on conductive substrates.<sup>13-15</sup> It has already been utilized to prepare coatings on biosensor, bioelectrode and endosseous implant.<sup>16, 17</sup> Our previous studies also demonstrated that EPD was an effective technique to prepare chitosan-gelatin (CSG) composite coating on Ti substrate, and this CSG coating was a promising candidate for further loading of functional agents.<sup>18, 19</sup> The CSG coating was prepared under mild conditions (room temperature, and water as the solvent), and there was no specific requirement for the shape and structure of the substrate. It showed favourable mechanical property, biodegradability and biocompatibility. However, it is still unknown if functional agents can be loaded into the CSG coating, how to load them into the coating, and if functional effects of the loaded agents could be preserved.

To explore this application and its mechanism, tetracycline (Tc) was chosen as the model functional agent. It is a kind of wide spectrum antibiotic and cationic drug. Due to its fluorescence and high affinity to mineralized tissue, Tc can be easily detected for the entrapment and release assay, and used as a marker for topical drug release in bone tissue.<sup>20, 21</sup> Moreover, under the influence of high temperatures, light, and acidic conditions, decomposition reactions of Tc can take place, and inactivate its fluorescence and antibacterial effect. Therefore, Tc is a suitable model drug to evaluate the loading of functional agents in CSG coatings.<sup>22</sup> In addition, since Tc will be affected by electric current and pH change during EPD process, the preservation of Tc's functional effects after EPD is still uncertain.

In the present study, CSG nanosphere coating was fabricated on titanium substrate *via* EPD. Tc, as a model functional agent, was loaded into the coating during fabrication. The mechanism of fabricating Tc loaded CSG nanosphere coatings *via* EPD was investigated for the first time. The characterization of Tc loaded CSG coatings, as well as the preservation of Tc's antibacterial effect was investigated. Also, the nanosphere structure of the CSG based coating was revealed for the first time, while it was considered to be merely a membrane in our previous studies. This study would lead us to a more thorough understanding of the mechanism of fabricating Tc loaded CSG nanosphere coating *via* EPD, and facilitate the application of functional agents loaded CSG nanosphere coatings in surface functionalization of biomedical metallic materials.

## Experimental

### Materials

Chitosan (MW 1,000,000, humidity 7.86%, ash content 0.80%, deacetylation degree greater than 95%) was supplied by Golden-Shell Pharmaceutical Co., Ltd (Zhejiang, China). Gelatin (type A) and tetracycline hydrochloride (Tc) were obtained from Sigma (Buchs, Switzerland). Commercial pure titanium

(grade 2) was supplied by Baoji Titanium industry Co., Ltd and prepared according to our previous study.<sup>18</sup> Bacterial strains of *Staphylococcus aureus* (*S. aureus*; ATCC 25923) and *Escherichia coli* (*E. coli*; ATCC 25922) were obtained from American Type Culture Collection. All the other chemical reagents were local products of analytical grade.

### Preparation and characterization of electrophoretic solutions

The electrophoretic solutions were prepared according to our previous article.<sup>18</sup> In brief, 1.2 g chitosan was dissolved in 150 mL of 0.04 M hydrochloric acid (HCl) solution and filter sterilized with 0.45  $\mu\text{m}$  Millipore filter (Bedford, MA). Then 2.8 g gelatin powder was dissolved into chitosan solution at 60 °C for 1.5 h. After that, Tc powder was dissolved into the blend solution at room temperature. All solutions were adjusted to pH 4.0 using 0.1 M sodium hydroxide (NaOH) and then brought to a total volume of 200 mL with Milli-Q water. Blends containing 0, 1 and 10 mg/mL Tc were produced and coded here as CSG, Tc1, and Tc10, respectively. All work was done under aseptic condition.

Zeta potential of each electrophoretic solution was measured by photon correlation spectroscopy ( $n=3$ ) (Zetasizer 3000, Malvern Instruments, UK). For transmission electron microscopic (TEM) analysis, the electrophoretic solutions were diluted 100 times with HCl or NaOH solution, pH values were kept to 4 or 10, respectively. As to the observation of released nanosphere, each coating was immersed in 5 mL PBS solution for 24 hours, then the soaking solution was diluted 5 times with Milli-Q water. Followed by ultrasonic dispersion, samples were dropped on the surface of copper grid and dehydrated before observation using TEM (JEOL JEM 2010, JEOL Ltd., Japan).

### EPD process

During EPD process, Ti substrate was used as cathode and parallel platinum plate as counter electrode, with 50 mm in between. Deposition was performed using a direct current power supply (Model 6614C, Agilent Technologies, China) with a constant voltage of 5 V  $\text{cm}^{-2}$  for 2.5 min. After deposition, the cathode was removed from electrophoretic solution, rinsed with Milli-Q water, and air-dried on a clean bench under dark condition overnight.

### Characterization of the nanosphere coatings

After EPD, the coatings were visualized by inverted fluorescence microscopy (Nikon TE-2000) with a CCD camera (Spot Diagnostic Instruments Inc.). After air dried, optical photographs of the coatings were taken. Surface morphology was observed by scanning electron microscope (SEM; Fei Quanta-200, Netherlands). Surface chemistry was investigated with attenuated total reflection Fourier transform infrared spectroscopy (ATR-FTIR; Thermo Nicolet 5700, USA). X-ray diffraction (XRD) and micro-area XRD patterns were measured using an X-ray Diffractometer (Bruker Axs D8 Advance, Karlsruhe, Germany) under a voltage of 30 kV and 30 mA using Cu K $\alpha$  radiation. The diffraction pattern was determined over a

range of diffraction angle  $2\theta = 5^\circ$  to  $2\theta = 60^\circ$  at a rate of  $1^\circ$  ( $2\theta$ ) per min and a step size of  $0.1^\circ$  ( $2\theta$ ).

To investigate the coating-titanium interface, shear bond strength test was performed according to our previous study.<sup>18</sup> In brief, the coating surface was adhered to another titanium plate using instant gel adhesive, and cured for 24 hours at room temperature. The pull test was conducted using an electrical mechanical Instron Model 4465 load frame (Instron Corporation, Norwood, MA) with a 5000N load cell. It was run at a constant crosshead displacement of 0.50 mm per min until failure was reached as it was evidenced by a drop in load ( $n = 5$ ).

#### Tc entrapment and release assays

For Tc entrapment assay, Tc was recovered from Tc1 and Tc10 coatings by incubating each coating in 5 mL 0.1M NaOH at room temperature for 2 h ( $n = 3$ ). Absorbance value of the immersion solution at 350 nm was measured using a Unicam UV500 spectroscopy (Thermo Spectronic, Cambridge, UK). Absorbance/Tc concentration calibration curve was established using a series of Tc-NaOH solutions ranging from 0.1 to 10 mg/mL at 350 nm.

For Tc release assay, each sample was placed in 15 mL PBS solution without agitation and incubated at  $37^\circ\text{C}$  for up to 24 hours under dark condition. At pre-determined time intervals, 1 mL immersion solution was extracted, then 1mL fresh PBS was added to the release system. Absorbance value of the immersion solution was measured at 350 nm. Absorbance/Tc concentration calibration curves of each time point were established using serially diluted PBS-Tc solutions ranging from 0.01 to 0.1 mg/mL at 350 nm to eliminate the influence of Tc attenuation.

#### Antibacterial study

*S. aureus* and *E. coli* were cultured in tryptic soy broth (TSB) and Luria-Bertani (LB) medium at  $37^\circ\text{C}$  on a shaker bed at 200 rpm for 4 - 6 h, respectively. Then the concentration was adjusted to  $1 \times 10^6$  colony-forming units (CFUs)/mL and spread evenly on TSB or LB agar plates. Ti discs with and without coatings were placed on the above prepared agar plates separately, incubated at  $37^\circ\text{C}$  for 24 hours and photographed to record the zones of inhibition (ZOI). For quantitative assay of viable bacteria cells, aforementioned samples ( $n = 3$ ) were immersed in 2 mL bacteria suspension and shaken at 100 rpm at  $37^\circ\text{C}$  for 3 h. The substrates were removed with sterile forceps and gently washed with 5 mL sterile PBS. The bacteria suspension and PBS were collected for bacterial counting. The substrates were then placed in broth, and the bacteria retained on substrates were dislodged by mild ultrasonication (for 6 min) in a 100 W ultrasonic bath operating at a nominal frequency of 50 Hz, followed by rapid vortex mixing (10 s). Serial 10-fold dilutions were performed and viable counts were estimated following the spread plate method.<sup>23</sup> The number of CFU on each plate was counted and expressed relatively to the surface area of culture plate ( $\text{CFU}/\text{cm}^2$ ).

#### Statistical analyses

**Table 1.** Initial composition of the electrophoretic solution and drug entrapment

Formulation	CSG	Tc1	Tc10
Chitosan	0.3 g	0.3 g	0.3 g
Gelatin	0.7 g	0.7 g	0.7 g
Milli-Q water	50 mL	50 mL	50 mL
Tetracycline hydrochloride	0	50 mg	500 mg
Drug entrapped $\pm$ SD	0	$100 \pm 3 \mu\text{g}$	$704 \pm 34 \mu\text{g}$

Quantitative data were expressed as means  $\pm$  standard deviation. Statistical analysis was carried out by one-way analysis of variance (ANOVA) and post hoc testing for the following measurements, for which differences were considered significant at  $p < 0.05$ .

## Results and Discussion

### The mechanism of EPD

To create Tc loaded CSG nanosphere coating, we employed a EPD approach, wherein chitosan and gelatin were initially dissolved in HCl, then Tc (as a functional additive) was added to the CSG solution in a dose-dependent manner (Table 1). After that, EPD was conducted using Ti substrate as cathode, then the Tc loaded CSG nanosphere coating was fabricated on Ti substrate. The weight to weight ratio of chitosan to gelatin in the electrophoretic solution was 3:7, which was based on our previous study that showed this ratio group had the best mechanical property and biological response of pre-osteoblasts.<sup>18</sup> The colour of electrophoretic solution became more yellow with the growing amount of Tc (Figure 1A).

To explore the mechanism of EPD and characterize the nanosphere coating, zeta potential and TEM analyses were applied. Chitosan is a linear polysaccharide, which has primary amino groups with  $pK_a$  value around 6.3.<sup>24</sup> It was positively charged with zeta potential about +52.7 mV in HCl solution ( $\text{pH} = 4$ ). Gelatin (type A) has high content of amino acids glycine, and the  $pK_a$  value is around 6.1.<sup>25</sup> It was also positively charged with zeta potential about +11.8 mV when  $\text{pH} = 4$ . Tetracycline has three  $pK_a$  values, which are approximately 3.3, 7.7 and 9.7 for tricarbonylamide, phenolic diketone, and dimethylamine groups, respectively. This characteristic makes tetracycline existing as a cationic, zwitterionic, and anionic species under acidic, moderately acidic to neutral, and alkaline conditions, respectively.<sup>26, 27</sup> It was also positively charged with zeta potential about +41.1 mV when  $\text{pH} = 4$ . Therefore, in the electrophoretic solution, chitosan, gelatin and Tc were all positively charged and formed a stable and homogeneous colloid system (Figure 1D1).

According to literature, pH value around the cathode will rise up to 10 during EPD process.<sup>28</sup> In order to mimic this pH change, we adjusted the pH value of electrophoretic solution from 4 to 10, then observed it using TEM (Figure 1C). Results showed amorphous structure in CSG and Tc1 groups, and very small particles could be found in Tc1 and Tc10 groups when  $\text{pH} = 4$  (Figure 1C1 – 1C3). When  $\text{pH} = 10$ , nanospheres could be

found in all 3 groups, the diameters were: 10 - 51 nm for CSG group (Figure 1C4); 24 - 124 nm for Tc1 group (Figure 1C5); and 59 - 443 nm for Tc10 group (Figure 1C6). Additionally, each coating was immersed in 5 mL PBS for 24 h, then the soaking solution was observed using TEM. Nanospheres could be found in the soaking solution, they were homogeneously distributed in CSG group (Figure 1C7), and accumulated near the wall of copper TEM grid after Tc incorporation (Figure 1C8 and 1C9). These results confirmed the nanosphere structure in CSG coatings, and indicated that the nanospheres were formed during pH change near the cathode. Moreover, they could be released from the coatings in PBS after 24 hours' immersion. According to literature, the use of nano-carriers for drug delivery was believed to improve the therapeutics' solubility, extend their half-life, improve their therapeutic index, and reduce their immunogenicity.<sup>29</sup> Thus, compared with polymer network or hydrogel coatings, the CSG nanosphere coatings might be considered as an advanced and promising surface functionalization strategy for biomedical metallic materials.

Therefore, the mechanism of fabricating Tc loaded CSG nanosphere coating *via* EPD can be summarized as: (1) Before voltage was applied, the electrophoretic solution was in a stable and homogeneous colloid form because of the electrostatic repulsion among the positively charged ingredients (Figure 1D1). (2) After voltage was applied for a certain time, pH value near the cathode rose up to 10. The positively charged ingredients concentrated around the cathode under the influence of electric current (Figure 1D2). (3) Near the cathode, chitosan, gelatin and tetracycline experienced a higher pH than their  $pK_a$  values. Most of chitosan's amino groups were deprotonated and became insoluble. Gelatin became negatively charged due to  $-COO^-$  groups. Tetracycline also became negatively charged, because its hydroxyl groups became negative and the C-4 nitrogen deprotonated.<sup>27</sup> Therefore, electrostatic interaction among  $-NH_3^+$  groups carried on chitosan,  $-COO^-$  groups on gelatin, and negatively charged hydroxyl groups on Tc took place and formed a nanosphere structure. Since chitosan was insoluble near the cathode, Tc loaded CSG nanosphere coating could be deposited onto the titanium substrate. Meanwhile, Tc could be physically entrapped into the coating, which would be another possible mechanism of Tc loading. (Figure 1D3).

#### Characterization of the nanosphere coatings

**Topography description.** In this study, CSG nanosphere coatings were successfully prepared on Ti substrates *via* EPD. The optical photographs showed that coatings were uniformly deposited on Ti substrate. After the nanosphere coated Ti disks were air dried, the coatings presented a thin film like structure on Ti disks. The yellowish colour became thicker with growing amount of Tc in the coatings (Figure 2A - D). Fluorescence images presented that all coatings had similar macro-porous structure, with pore size ranging from 50 to 400  $\mu m$  (Figure 2E - H). The porosity was produced by gas bubbling at the electrode and by elimination of water from the gel. It has been reported that porous structure benefits cell growth,

migration and nutrient flow. Scaffolds with pore size ranging from 200 - 500  $\mu m$  were favourable towards bone ingrowth *in vivo*,<sup>30</sup> thus satisfactory *in vivo* performance of our nanosphere coatings could be expected. Since Tc has a bright yellow fluorescence, it can be easily detected under fluorescent microscope, which makes it a suitable model drug in this study. Similar to the optical images, the yellow fluorescence became brighter with growing amount of Tc in the coatings (Figure 2E - H). In addition, yellow crystals could be found in Tc10 group (Figure 2H). Low magnification SEM micrographs showed that the pore walls of CSG coating were relatively intact (Figure 2J). Some cracks and fissures appeared on that of Tc1 and Tc10 coatings (Figure 2K, L). High magnification SEM micrographs displayed nanosphere-like structure embedded in the membrane, especially in Tc1 and Tc10 groups (Figure 2O, P).

**ATR-FTIR analysis.** According to our previous study,<sup>18</sup> chitosan displayed strong absorption peaks at 1151, 1083, and 1033  $cm^{-1}$ , which were characteristic peaks of a polysaccharide structure due to C-N stretching, C-O stretching, and O-H bending. Gelatin showed strong absorption peaks at 1638 and 1548  $cm^{-1}$  due to amide I,  $-CONH-$  stretching, and amide II,  $-NH_2$  stretching, respectively. Tc powder displayed the peaks of amide bond structure in benzene ring at 1668, 1520 and 1227  $cm^{-1}$ . It also showed the distinctive peaks of carbonyl groups in benzene ring at 1614 and 1581  $cm^{-1}$ , and the C=C skeleton vibration at 1449  $cm^{-1}$  (Figure 3D).

ATR-FTIR spectrum of the nanosphere coatings demonstrated that chitosan and gelatin were both deposited onto CSG and Tc1 coatings, and both of them showed similar FTIR spectrum (Figure 3A, B). The absorption peak of tetracycline could not be detected in Tc1 group, because tetracycline content in the coating was very low. As for Tc10 group, the absorption peaks of chitosan were missing. But they could be retrieved after 3 hours' immersion in PBS, where the yellow crystals on Tc10 coating were dissolved in PBS (data not shown). Thus, it could be hypothesised that the yellow crystals on Tc10 coating (Figure 2) covered the absorption peaks of chitosan. The amide II band tended to shift to lower wavenumber at about 1504  $cm^{-1}$  (Figure 3C), which might indicate the weakening of hydrogen bonds between the amino and carbonyl groups in the backbone of gelatin.<sup>31,32</sup> Meanwhile, the absorption peaks of amide bond structure in benzene ring of Tc shifted to lower wavenumber (from 1520  $cm^{-1}$  to 1504  $cm^{-1}$ ). Therefore, we suggested that new hydrogen bonds were formed between the peptide amino and carbonyl groups in the backbone of gelatin and amide group in benzene ring of Tc.

**XRD Analysis.** The XRD pattern of chitosan powder displayed diffraction peaks at  $2\theta = 11.6^\circ$  and  $20.1^\circ$  (Figure 4D). For gelatin powder, the diffraction peaks were  $2\theta = 7.7^\circ$  and  $21.4^\circ$  (Figure 4E). Tc powder showed crystalline structure with  $2\theta$  scattering angle ranging from  $8.7^\circ$  to  $35^\circ$  (Figure 4F). For all the nanosphere coating groups, the peaks of chitosan became lower and broader, which indicated that chitosan in all coatings was predominantly in amorphous form (Figure 4A - C). Also, previous study showed that chitosan in composite coatings prepared *via* EPD was in amorphous form.<sup>33</sup> In Tc10 group (Figure 4C), diffraction peak at  $2\theta = 8.3^\circ$  indicated that

the crosslink of gelatin with Tc may influence the direction of crystal growth of the nanosphere coating, where typical crystallization peak of gelatin coating is at around  $2\theta = 8.0^\circ$ .<sup>34</sup> The reflection peaks at  $2\theta = 26.7^\circ, 35.3^\circ, 38.5^\circ, 40.2^\circ$  and  $53.1^\circ$  corresponded to the Ti substrate.

To further investigate the crystal structure of the nanosphere coatings, CSG and Tc10 coatings were analysed by micro-XRD: one point was chosen on CSG coating, another point was chosen on the crystals of Tc10 coating, the last point was chosen on the coating surface without crystal of Tc10 coating (Figure 5). Results showed typical gelatin peak ( $2\theta = 7.6^\circ - 8.2^\circ$ ) in all three points (Figure 5A - C). After incorporation of Tc, this peak became higher and narrower, which indicated that the crosslink of gelatin with Tc would increase the crystallinity of the nanosphere coating.

**Mechanical test.** At the end of the shear bond strength test, all coatings were detached from titanium substrates. The failures occurred at the coating-titanium interface rather than coating-gel adhesive interface. Figure 6 showed the results of shear bond strength test, and its schematic diagram. The mean shear bond strength of CSG, Tc1 and Tc10 coatings were 3.5, 4.5 and 16.0 MPa, respectively. Statistical analysis indicated that Tc10 group had significantly higher shear bond strength than CSG and Tc1 groups, with no statistic difference between CSG and Tc1 group. This significantly elevated mechanical property might result from the increased crystallinity of the Tc-incorporated CSG coating. Similar trend has also been reported that chitosan and gelatin based edible films with higher molecular ordering and crystallinity resulted in higher tensile strength and modulus.<sup>35</sup> Therefore, the addition of Tc could increase the crystallinity, and may also increase the ordering of crystal structure in CSG coatings, which resulted in the enhanced mechanical interlocking between coating and titanium surface.

#### Tc entrapment and release study

The amount of Tc entrapped in each sample was  $100 \pm 3 \mu\text{g}$  for Tc1 group, and  $700 \pm 34 \mu\text{g}$  for Tc10 group (Table 1), which indicated that the entrapment of Tc depended on the initial drug concentration in electrophoretic solution. Since a relatively small titanium plate was used as cathode in the vast amount of electrophoretic solution, the drug entrapment seems lower than those using simple absorption methods.<sup>36,37</sup> But the present system could continuously prepare more than 10 CSG coatings in a row, without detectable difference among samples. Upon EPD, Tc was chemically bonded to gelatin, which was supported by ATR-FTIR results. Meanwhile, Tc was concentrated around the cathode, enabling its physical entrapment into the nanosphere coating.

For the Tc release study, Tc was almost completely released after 3 hours of incubation. Then the accumulated amount of released Tc became lower with longer incubation time, which might be explained by the resorption of Tc from immersion solution to the coating (Figure 7).<sup>38</sup> Although sustained release was preferred for drug delivery because of the short half-lives of most drugs and renal clearance,<sup>39</sup> this burst release profile could ensure high drug concentration in topical area in a short

time, which prevented low topical drug concentration and side effects of systemic application. In addition, since nanosphere could also be released from the coatings in TEM analysis, function mode of the nanosphere coating could be: direct release of Tc, release of CSG-Tc nanosphere, or a combination of both. Therefore, sustained release of functional agents from the CSG nanosphere coating together with the exact function mode of the coating still needs further investigation.

#### Antibacterial study

One of the most serious drawbacks of conventional coating methods is the loss of biological function after preparation, because of severe preparation conditions, such as high temperature, organic solvent and radiation.<sup>40,41</sup> The advantage of EPD is mild preparation condition which could preserve the biological function: it is prepared in water (with no organic solvent), at room temperature or even  $4^\circ\text{C}$ .<sup>42,43</sup> However, the electric current and pH change near the cathode during EPD process may still affect the loaded functional agents. In order to verify the preservation of Tc's functional effects after EPD, antibacterial experiments were performed.

The antibacterial experiments were carried out with *S. aureus* and *E. coli*, the most common Gram-positive and Gram-negative microbial pathogen encountered in biomaterial-associated infections, respectively.<sup>44</sup> For the ZOI test, both Tc1 and Tc10 groups showed clear ZOI around the samples after 24h incubation with *S. aureus* or *E. coli*, while none of Ti and CSG group showed ZOI (Figure 8A and 8D). In addition to the qualitative ZOI test, quantitative determination of viable bacteria cells on these substrates and in the suspension was conducted using the spread plate method,<sup>23</sup> with the results shown in Figure 8. For *S. aureus*, all Ti, Tc1 and Tc10 groups showed significantly reduced suspended bacterial cell number than CSG group (Figure 8B), while CSG, Tc1 and Tc10 groups showed significantly reduced adherent bacterial cell number than Ti group (Figure 8C). For *E. coli*, Tc10 group showed significantly reduced suspended and adherent bacterial cell number than Ti and CSG groups (Figure 8E, F).

Consequently, these results confirmed that the antibacterial effect of Tc was preserved after EPD, especially for Tc10 group, which would provide evidential support for further loading of functional agents into the CSG nanosphere coatings. In general, incorporation of Tc reduced both adherent and suspended bacterial cell number. It can kill the bacteria adhered to the coating surface, then prevent biofilm formation, which is the most common cause of implant-related persistent infection.<sup>45</sup> Meanwhile, it can inhibit the bacteria in micro-environment, then remove the bacterial infection completely. Interestingly, CSG group showed significant higher suspended bacterial cell number of *S. aureus* (Figure 8B), and significant higher adherent and suspended bacterial cell number of *E. coli* (Figure 8E, F) than other groups. This could be explained by the release of gelatin from the coating, which contains RGD like sequences that promote cell adhesion, migration, and proliferation.<sup>46</sup>

## Conclusions

Based on our findings, and within the limitations of this study, it can be concluded that Tc loaded CSG nanosphere coating can be successfully fabricated on titanium substrate *via* EPD. Characterization of the coating showed nanosphere structure, and nanospheres could be released from the coating. The entrapment of Tc was confirmed by fluorescent microscope, Fourier transform infrared spectroscopy and X-ray diffraction pattern. Results also indicated new hydrogen bonds formed between Tc and gelatin, as well as the increased crystallinity of the nanosphere coating. Mechanical test demonstrated enhanced mechanical interlocking in the coating-titanium interface of high Tc concentration group. Although Tc was released from the coating with a burst release profile, its antibacterial effect was preserved after coating preparation both qualitatively and quantitatively.

Additionally, incorporation of CSG nanosphere coating with other functional agents, such as anticancer, gene segment, amino acid and metallic ions, will contribute to our understanding and further application of this CSG nanosphere coating. The functionalized CSG nanosphere coating could be a promising surface functionalization strategy for biomedical metallic materials.

## Acknowledgements

This work was financially supported by National Natural Science Foundation of China (No. 81470771, 81371170 and 81200812), Fundamental Research Funds for the Central Universities (No. 2042014kf00232) and Doctoral Fund of Ministry of Education of China (No. 20120141130009).

## Notes and references

- M. Niinomi, *Metallurgical and Materials Transactions a-Physical Metallurgy and Materials Science*, 2002, **33**, 477-486.
- T. Hanawa, *Sci. Technol. Adv. Mater.*, 2012, **13**.
- K. Alvarez and H. Nakajima, *Materials*, 2009, **2**, 790-832.
- L. L. Hench and J. M. Polak, *Science*, 2002, **295**, 1014-1017.
- T. W. Hambley, *Dalton Trans.*, 2007, DOI: 10.1039/b706075k, 4929-4937.
- F. Variola, F. Vetrone, L. Richert, P. Jedrzejowski, J. H. Yi, S. Zalzal, S. Clair, A. Sarkissian, D. F. Perepichka, J. D. Wuest, F. Rosei and A. Nanci, *Small*, 2009, **5**, 996-1006.
- J. J. Gao, C. X. Li, J. F. Zhou, L. Q. Lu, C. J. Zhao and Y. C. Zhu, *Rsc Adv*, 2015, **5**, 20357-20364.
- M. Hirota, T. Hayakawa, M. Yoshinari, A. Ametani, T. Shima, Y. Monden, T. Ozawa, M. Sato, C. Koyama, N. Tamai, T. Iwai and I. Tohnai, *Int. J. Oral Maxillofac. Surg.*, 2012, **41**, 1304-1309.
- P. H. Chua, K. G. Neoh, E. T. Kang and W. Wang, *Biomaterials*, 2008, **29**, 1412-1421.
- M. Schuler, D. Trentin, M. Textor and S. G. Tosatti, *Nanomedicine*, 2006, **1**, 449-463.
- Y. Z. Yang, K. H. Kim and J. L. Ong, *Biomaterials*, 2005, **26**, 327-337.
- L. T. de Jonge, S. C. Leeuwenburgh, J. G. Wolke and J. A. Jansen, *Pharm. Res.*, 2008, **25**, 2357-2369.
- S. A. Hasan, J. L. Rigueur, R. R. Harl, A. J. Krejci, I. Gonzalo-Juan, B. R. Rogers and J. H. Dickerson, *ACS Nano*, 2010, **4**, 7367-7372.
- S. Seuss and A. R. Boccacini, *Biomacromolecules*, 2013, **14**, 3355-3369.
- L. V. Kovalev, M. V. Yarmolich, M. L. Petrova, J. Ustarroz, H. A. Terryn, N. A. Kalanda and M. L. Zheludkevich, *ACS Appl. Mater. Interfaces*, 2014, **6**, 19201-19206.
- X. L. Luo, J. J. Xu, J. L. Wang and H. Y. Chen, *Chem. Commun.*, 2005, DOI: Doi 10.1039/B419197h, 2169-2171.
- K. M. Gray, B. D. Liba, Y. Wang, Y. Cheng, G. W. Rubloff, W. E. Bentley, A. Montembault, I. Royaud, L. David and G. F. Payne, *Biomacromolecules*, 2012, **13**, 1181-1189.
- T. Jiang, Z. Zhang, Y. Zhou, Y. Liu, Z. Wang, H. Tong, X. Shen and Y. Wang, *Biomacromolecules*, 2010, **11**, 1254-1260.
- K. Ma, X. Cai, Y. Zhou, Z. Zhang, T. Jiang and Y. Wang, *Biomed. Mater.*, 2014, **9**, 015008.
- J. Slots and T. E. Rams, *J. Clin. Periodontol.*, 1990, **17**, 479-493.
- D. Wang, S. C. Miller, L. S. Shlyakhtenko, A. M. Portillo, X. M. Liu, K. Papangkorn, P. Kopekova, Y. Lyubchenko, W. I. Higuchi and J. Kopecek, *Bioconjugate Chem.*, 2007, **18**, 1375-1378.
- M. Kuhne, D. Ihnen, G. Moller and O. Agthe, *Journal of veterinary medicine. A, Physiology, pathology, clinical medicine*, 2000, **47**, 379-384.
- Z. Shi, K. G. Neoh, E. T. Kang and W. Wang, *Biomaterials*, 2006, **27**, 2440-2449.
- P. Sorlier, A. Denuziere, C. Viton and A. Domard, *Biomacromolecules*, 2001, **2**, 765-772.
- S. Azarmi, Y. Huang, H. Chen, S. McQuarrie, D. Abrams, W. Roa, W. H. Finlay, G. G. Miller and R. Lobenberg, *J. Pharm. Pharm. Sci.*, 2006, **9**, 124-132.
- C. Gu and K. G. Karthikeyan, *Environ. Sci. Technol.*, 2005, **39**, 2660-2667.
- L. J. Leeson, J. E. Krueger and R. A. Nash, *Tetrahedron Lett.*, 1963, **4**, 1155-1160.
- Y. Cheng, X. L. Luo, J. Betz, S. Buckhout-White, O. Bekdash, G. F. Payne, W. E. Bentley and G. W. Rubloff, *Soft Matter*, 2010, **6**, 3177-3183.
- R. A. Petros and J. M. DeSimone, *Nat Rev Drug Discov*, 2010, **9**, 615-627.
- S. J. Hollister, *Nat. Mater.*, 2005, **4**, 518-524.
- E. S. Manas, Z. Getahun, W. W. Wright, W. F. DeGrado and J. M. Vanderkooi, *J. Am. Chem. Soc.*, 2000, **122**, 9883-9890.
- Z. Zhang, Y. Y. Qu, X. S. Li, S. Zhang, Q. S. Wei, Y. S. Shi and L. L. Chen, *Appl. Surf. Sci.*, 2014, **303**, 255-262.

33. I. Zhitomirsky and A. Hashambhoy, *J. Mater. Process. Technol.*, 2007, **191**, 68-72.
34. Y. Rao, *Polymer*, 2007, **48**, 5369-5375.
35. I. S. Arvanitoyannis, A. Nakayama and S.-i. Aiba, *Carbohydr. Polym.*, 1998, **37**, 371-382.
36. F. Ungaro, I. d'Angelo, C. Coletta, R. d'Emmanuele di Villa Bianca, R. Sorrentino, B. Perfetto, M. A. Tufano, A. Miro, M. I. La Rotonda and F. Quaglia, *J. Control. Release*, 2012, **157**, 149-159.
37. M. H. Alkhraisat, C. Rueda, J. Cabrejos-Azama, J. Lucas-Aparicio, F. T. Marino, J. Torres Garcia-Denche, L. B. Jerez, U. Gbureck and E. L. Cabarcos, *Acta Biomater.*, 2010, **6**, 1522-1528.
38. A. Dashti, D. Ready, V. Salih, J. C. Knowles, J. E. Barralet, M. Wilson, N. Donos and S. N. Nazhat, *Journal of biomedical materials research. Part B, Applied biomaterials*, 2010, **93**, 394-400.
39. P. Gao, X. Nie, M. Zou, Y. Shi and G. Cheng, *J. Antibiot.*, 2011, **64**, 625-634.
40. L. G. Griffith and G. Naughton, *Science*, 2002, **295**, 1009-+.
41. M. Biondi, F. Ungaro, F. Quaglia and P. A. Netti, *Adv. Drug Del. Rev.*, 2008, **60**, 229-242.
42. T. H. Chen, D. A. Small, L. Q. Wu, G. W. Rubloff, R. Ghodssi, R. Vazquez-Duhalt, W. E. Bentley and G. F. Payne, *Langmuir*, 2003, **19**, 9382-9386.
43. Z. Zhang, T. Jiang, K. Ma, X. Cai, Y. Zhou and Y. Wang, *J. Mater. Chem.*, 2011, **21**, 7705-7713.
44. A. G. Gristina and J. W. Costerton, *J. Bone Joint Surg.-Am. Vol.*, 1985, **67**, 264-273.
45. R. O. Darouiche, *N. Engl. J. Med.*, 2004, **350**, 1422-1429.
46. Z. Guo, B. He, H. Jin, H. Zhang, W. Dai, L. Zhang, X. Wang, J. Wang, X. Zhang and Q. Zhang, *Biomaterials*, 2014, **35**, 6106-6117.

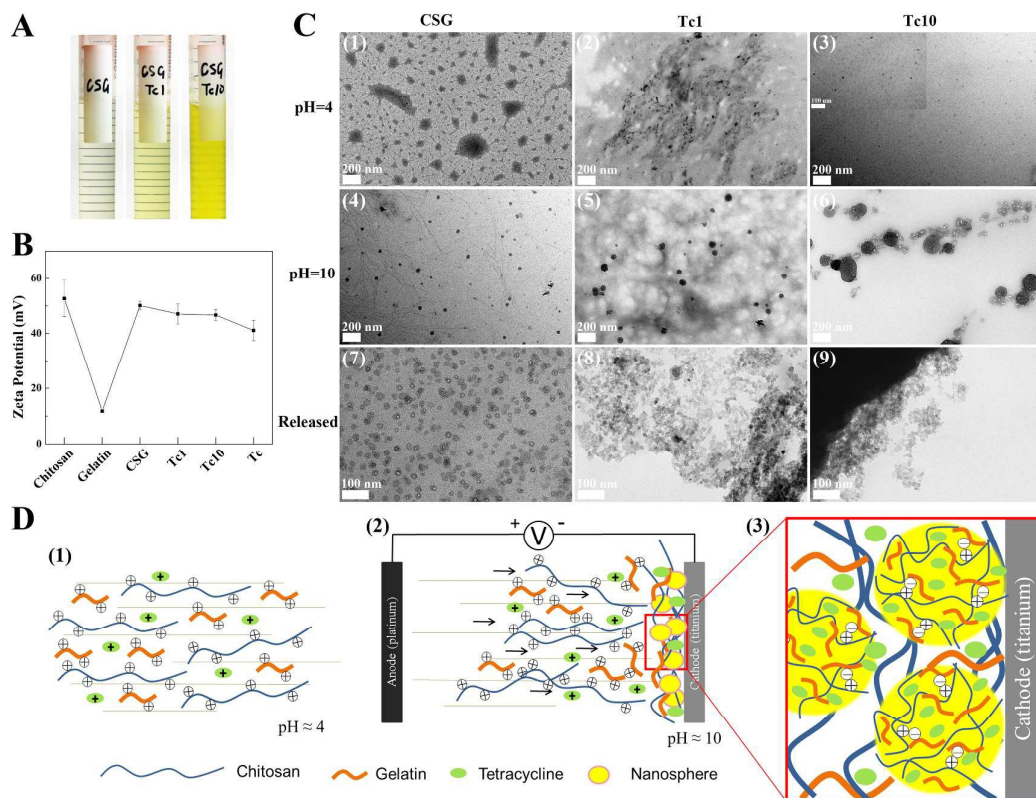


**Figure 1.** Characterization of the electrophoretic solutions and schematic diagram of the mechanism of EPD. (A) Optical images of the electrophoretic solutions. (B) Zeta potential of pure chitosan, pure gelatin, CSG, Tc1, Tc10 and pure Tc solutions. (C) TEM images of the electrophoretic solutions at pH = 4 (C1-C3) (higher magnification image were shown in the upper left corner of C3), pH = 10 (C4-C6), and the nanospheres released from the coatings (C7-C9). (D) Schematic diagram of the mechanism of EPD: when pH = 4, chitosan, gelatin and Tc were all positively charged in the electrophoretic solution (D1); after voltage was applied, CSG-Tc coating was deposited onto titanium substrate (D2); in the coating, CSG-Tc nanospheres were formed by electrostatic interaction (D3).

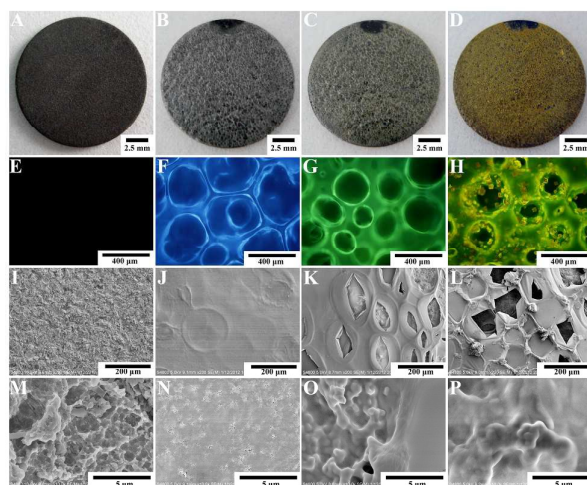


**Figure 2.** Representative optical photographs, fluorescence images, low magnification SEM images and high magnification SEM images of titanium substrate and different nanosphere coatings: (A, E, I, M) titanium substrate; (B, F, J, N) CSG coatings; (C, G, K, O) Tc1 coatings; (D, H, L, P) Tc10 coatings.

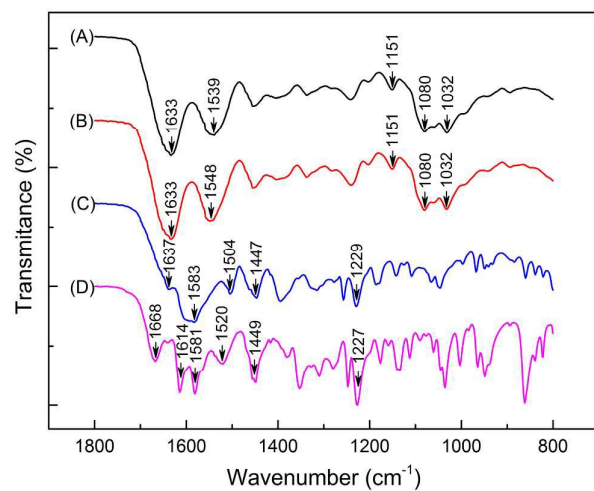
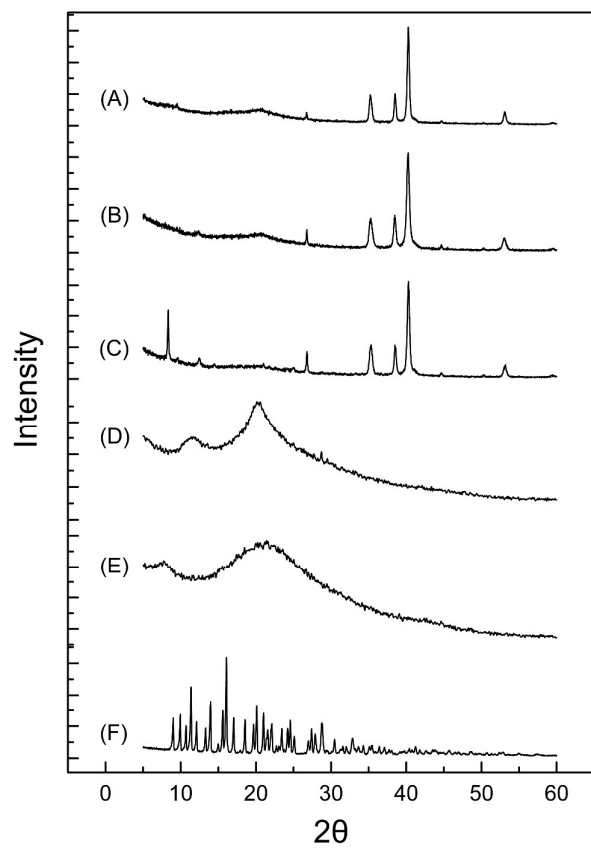
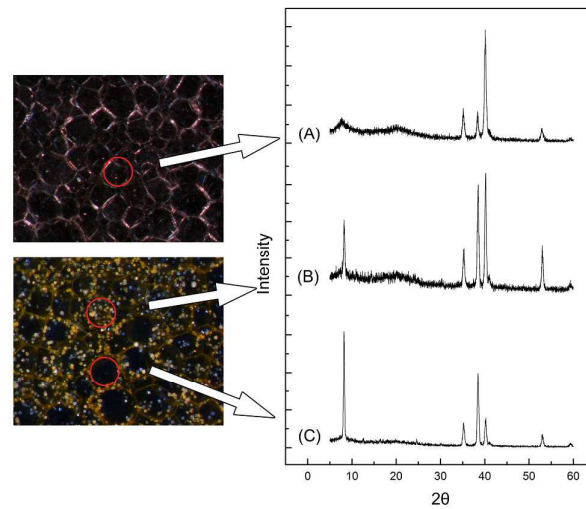


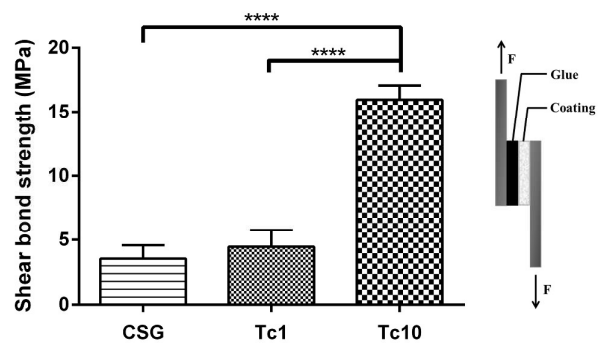
Figure 3. ATR-FTIR spectra of nanosphere coatings and Tc powder: (A) CSG coatings; (B) Tc1 coatings; (C) Tc10 coatings; (D) Tc powder.



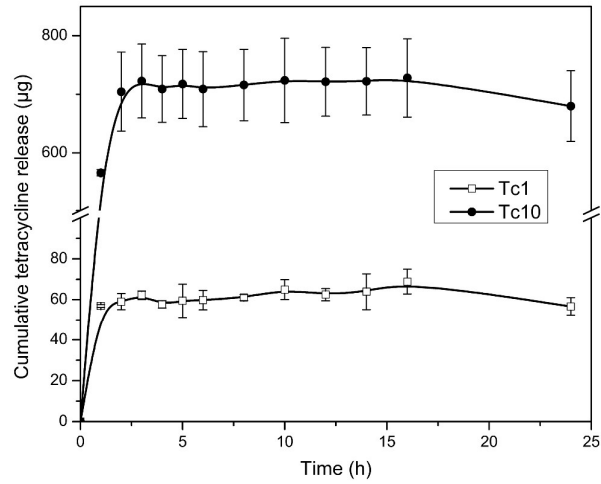
**Figure 4.** XRD patterns of coatings and their ingredients: (A) CSG coatings; (B) Tc1 coatings; (C) Tc10 coatings; (D) chitosan powder; (E) gelatin powder; (F) Tc powder.



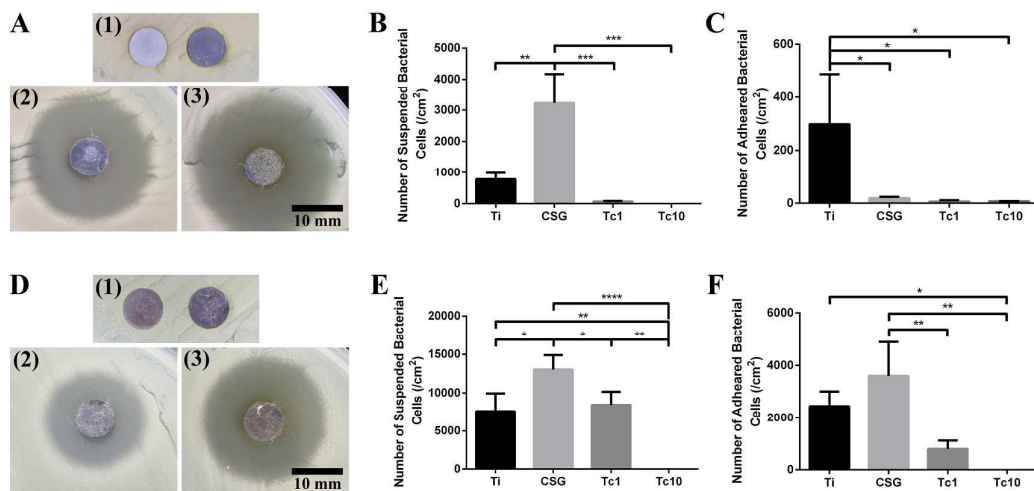
**Figure 5.** Micro-XRD patterns of CSG coatings (A), crystals on Tc10 coatings (B) and coating surface without crystal of Tc10 coatings (C). The optical photographs represent the scanning point of each micro-XRD pattern.



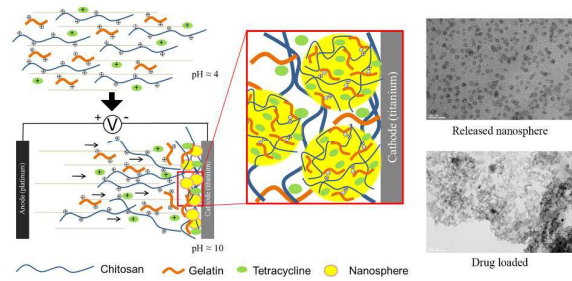
**Figure 6.** Bar graph and schematic diagram of the shear bond strengths of different coatings on titanium substrate. Error bar represent mean  $\pm$  SD for n = 5 (\*\*\*\* P < 0.001).



**Figure 7.** Cumulative release profiles of Tc released from Tc1 and Tc10 coatings in 15 mL PBS buffer.



**Figure 8.** Qualitative and quantitative analyses of antibacterial effect of different groups. (A) Zone of inhibition test against *S. aureus*: (1) titanium substrate and CSG coatings; (2) Tc1 coatings; (3) Tc10 coatings. (B) Number of viable adherent *S. aureus* cells on titanium substrate and nanosphere coatings. (C) Number of viable *S. aureus* cells in bacterial suspension cultured with different groups. (D) Zone of inhibition test against *E. coli*: (1) titanium substrate and CSG coatings; (2) Tc1 coatings; (3) Tc10 coatings. (E) Number of viable adherent *E. coli* cells on titanium substrate and nanosphere coatings. (F) Number of viable *E. coli* cells in bacterial suspension cultured with different groups (\*  $P < 0.05$ , \*\*  $P < 0.01$ , \*\*\*  $P < 0.005$ , \*\*\*\*  $P < 0.001$ ).



**Graphical Abstract:** Tetracycline loaded chitosan-gelatin nanosphere coating has been fabricate on titanium substrate via electrophoretic deposition.